Published May 23, 2024 as 10.3174/ajnr.A8357

Identification of a single-dose, low flip angle based CBV threshold for fractional tumor burden (FTB) mapping in recurrent glioblastoma

Aliya Anil, Ashley M. Stokes, John P. Karis, Laura C. Bell, Jennifer Eschbacher, Kristofer Jennings, Melissa A. Prah, Leland S. Hu, Jerrold L. Boxerman, Kathleen M. Schmainda, and C. Chad Quarles

ABSTRACT

BACKGROUND AND PURPOSE: DSC-MRI can be used to generate fractional tumor burden (FTB) maps, via application of relative CBV thresholds, to spatially differentiate glioblastoma recurrence from post treatment radiation effects (PTRE). Image-localized histopathology was previously used to validate FTB maps derived from a reference DSC-MRI protocol using preload, a moderate flip angle (MFA, 60°) and post-processing leakage correction. Recently, a DSC-MRI protocol with a low flip angle (LFA, 30°) with no preload was shown to provide leakage-corrected RCBV equivalent to the reference protocol. This study aims to identify the RCBV thresholds for the LFA protocol that generate the most accurate FTB maps, concordant with those obtained from the reference MFA protocol.

MATERIALS AND METHODS: Fifty-two patients with grade IV GBM who had prior surgical resection and received chemotherapy and radiotherapy were included in the study. Two sets of DSC-MRI data were collected sequentially first using LFA protocol with no preload, which served as the preload for the subsequent MFA protocol. Standardized relative CBV maps (sRCBV) were obtained for each patient and co-registered with the anatomical post-contrast T1-weighted images. The reference MFA-based FTB maps were computed using previously published sRCBV thresholds (1.0 and 1.56). An ROC analysis was conducted to identify the optimal, voxel-wise LFA sRCBV thresholds, and the sensitivity, specificity, and accuracy of the LFA-based FTB maps were computed with respect to the MFA-based reference.

RESULTS: The mean sRCBV values of tumors across patients exhibited strong agreement (CCC = 0.99) between the two protocols. Using the ROC analysis, the optimal lower LFA threshold that accurately distinguishes PTRE from tumor recurrence was found to be 1.0 (sensitivity: 87.77%; specificity: 90.22%), equivalent to the ground truth. To identify aggressive tumor regions, the ROC analysis identified an upper LFA threshold of 1.37 (sensitivity: 90.87%; specificity: 91.10%) for the reference MFA threshold of 1.56.

CONCLUSION: For LFA-based FTB maps, a sRCBV threshold of 1.0 and 1.37 can differentiate PTRE from recurrent tumor. FTB maps aids in surgical planning, guiding pathological diagnosis and treatment strategies in the recurrent setting. This study further confirms the reliability of single-dose LFA-based DSC-MRI.

ABBREVIATIONS: LFA = low flip angle; MFA = moderate flip angle; sRCBV = standardized relative cerebral blood volume; FTB = fractional tumor burden; PTRE = post treatment radiation effects; ROC = receiver operating characteristics; CCC = concordance correlation coefficient.

Received month day, year; accepted after revision month day, year.
From the Department of Cancer Systems Imaging (A.A., C.C.Q.), and Department of Biostatistics (K.J.), The University of Texas MD Anderson Cancer Center, Houston, Texas, United States; Division of Neuroimaging Research and Barrow Neuroimaging Innovation Center (A.M.S.), Department of Neuroradiology (J.P.K.), and Department of Neuropathology (J.E.), Barrow Neurological Institute, Phoenix, Arizona, United States; Clinical Imaging Group (L.C.B.), Genentech Inc., South San Francisco, California, United States; Department of Biophysics (M.A.P., K.M.S.), Medical College of Wisconsin, Milwaukee, Wisconsin, United States; Department of Radiology (L.S.H.), Mayo Clinic, Phoenix, Arizona, United States; Department of Diagnostic Imaging (J.L.B.), Rhode Island Hospital, Providence, Rhode Island, United States.

Laura C Bell is employed by Genentech Inc. Kathleen M. Schmainda has ownership interest in IQ-AI Ltd and Prism Clinical Imaging. Kathleen M. Schmainda has financial interest in Imaging Biometrics LLC. Kathleen M. Schmainda is a board member for Prism Clinical Imaging.
The remaining authors declare no conflicts of interest related to the content of this article.

This work was supported by National Institutes of Health/National Cancer Institute: R01 CA264992 (C.C.Q), U01 CA176110 (K.M.S), R01CA213158 (C.C.Q) and Cancer Prevention and Research Institute of Texas RR220038 (C.C.Q).

Please address correspondence to C. Chad Quarles, Ph.D., Department of Cancer Systems Imaging, The University of Texas MD Anderson Cancer Center, 1881 East Road, Unit 1907, Houston, Texas, 77054, United States; mailto:ccquarles@mdanderson.org.

SUMMARY SECTION

PREVIOUS LITERATURE: Cerebral blood volume maps derived from a DSC-MRI protocol using contrast agent preload, a moderate flip angle (60°), and post-processing leakage correction have been well-validated through image-guided histopathology and are recommended for clinical use. Recently, computational and in vivo patient studies demonstrated that the use of a low flip angle (30°) without a preload produces sRCBV maps in strong agreement to the double-dose reference protocol. Fractional tumor burden

Copyright 2024 by American Society of Neuroradiology.

maps, computed by applying sRCBV thresholds established by image-localized histopathology, enable reliable detection of regional tumor recurrence. This study aims to identify the sRCBV thresholds for the LFA protocol.

KEY FINDINGS: The mean and the voxel-wise tumor sRCBV values between the LFA and MFA protocol exhibited strong agreement. An ROC analysis identified two sRCBV thresholds for the LFA protocol to reliably differentiate treatment effects from tumor (1.0) and to identify regions with a high probability of viable tumor cells (1.37).

KNOWLEDGE ADVANCEMENT: FTB maps derived from the LFA protocol without the preload effectively distinguishes between tumor and treatment effects, affirming the reliability of a single-dose LFA-based DSC-MRI protocol. Nevertheless, it is essential to validate these thresholds using histopathology to facilitate their utilization in clinical decision-making.

INTRODUCTION

Glioblastoma (GBM) is an aggressive brain tumor associated with high degree of vascularity and malignancy. The standard treatment for GBM includes surgical resection followed by radiation therapy and chemotherapy with temozolomide (TMZ).[1] Conventional MRI scans taken 3-6 months after treatment often show new regions of enhancement, indicating the disruption of the blood brain barrier (BBB). This enhancement could be due to tumor recurrence or post treatment radiation effects (PTRE). Since both tumor recurrence and PTRE have similar visual appearance, conventional MRI scans are unable to reliably differentiate between the two.[2–5] Distinguishing between PTRE and tumor recurrence is crucial because they require different treatment management, since recurrence indicates treatment failure and PTRE signifies favorable treatment response, tumor stabilization and better prognosis.[6–9] Studies have demonstrated that advanced imaging techniques including perfusion-weighted and diffusion MRI, positron emission tomography (PET) and magnetic resonance spectroscopy (MRS), have the capability to differentiate between tumor and PTRE.[10–12] Among these advanced imaging techniques, perfusion-weighted MRI has been found to be effective in differentiating tumor recurrence from PTRE.[13–18]

Dynamic susceptibility contrast (DSC) MRI is a perfusion-based MRI method that provides information about tissue hemodynamics and vasculature. The relative cerebral blood volume (rCBV) derived from DSC-MRI is a useful noninvasive diagnostic tool that helps identify neoangiogenesis corresponding to high-grade glioma.[14,15,19–22] Commonly, rCBV maps are normalized to a normal appearing tissue region of interest (ROI) for ease of comparison across patients and time. More recently, this approach has been refined through standardization of rCBV maps (sRCBV). Unlike normalization, standardization translates the rCBV values to a standard intensity scale, removing the variability associated with user-dependent ROIs.[23] This increases consistency and enables quantitative comparison across studies, making it an important step in optimizing workflow and achieving consensus methodology.[24,25]

Image guided tissue histopathology and spatially matched rCBV data have been used to identify sRCBV thresholds that signify clinically relevant tissue states.[24,26,27] A sRCBV threshold of 1.0 can be used to differentiate tumor recurrence (sRCBV > 1.0) and PTRE (sRCBV < 1.0).[24,26,28] For regions with sRCBV > 1.0, an upper threshold has been used to further distinguish the degree of tumor vascularity. In a recent study, sRCBV was spatially matched to diagnostic tissue samples and it was determined that the probability of finding viable tumor in voxels was 71% for sRCBV > 1.0 based on ROC analysis and 88% for sRCBV > 1.56, which was the lower 95% CI for glioblastoma tissue samples.[27,29] The probability of tumor burden increases as the threshold increases. The application of these voxel-based thresholds to sRCBV maps enables generation of fractional tumor burden (FTB) maps defining three classes, containing colored voxels for each class: FTB_{low} (blue), percentage of voxels with sRCBV values < 1.0; FTB_{mid} (yellow), percentage of voxels with sRCBV values between 1.0 and 1.56; and FTB_{high} (red), percentage of voxels with sRCBV > 1.56.[24,26,29,30] FTB maps provide a spatial depiction of regional tumor recurrence and PTRE, as these can often coexist in varying degrees within a single lesion. FTB maps could aid in surgical planning, pathological diagnosis, and treatment planning in patients suspected of recurrence.

Multiple studies have shown that DSC-MRI, when acquired and post-processed using a standardized protocol, improves the correlation of rCBV with histopathology. This improvement bolsters the capability to differentiate tumor from PTRE, thereby influencing clinical decision-making.[31–35] The rCBV maps used for tissue validation were derived from the consensus recommended DSC-MRI protocol using a moderate flip angle (MFA; 65-75°), 25-35 ms TE, TR < 1.5 sec, full-dose contrast agent as preload, followed by full-dose contrast agent for bolus injection, and application of the Boxerman-Schmainda-Weisskoff (BSW) post-processing leakage correction method to minimize the confounding effects of contrast agent extravasation.[33,36–38] However, a second option was also included in the consensus recommendation. This option matches the protocol above except for the use of a low flip angle (30°), a field-strength dependent TE (45 ms at 1.5T and 30 ms at 3.0T) and removal of the contrast agent preload. In a multi-site validation study in patients with recurrent high-grade glioma, this single-dose option provided mean tumor sRCBV values that agreed with those derived from the double-dose protocol.[39] The use of the single-dose, low flip angle protocol (LFA) eliminates the potential error arising from variations in contrast agent incubation time and dosing. Although the mean tumor sRCBV values have been validated, there is a compelling need to establish the voxel-wise LFA-based rCBV thresholds needed for reliable FTB mapping.

The objective of this study is to determine the sRCBV thresholds for the LFA protocol which produce FTB maps that best match those derived from the previously validated double-dose MFA protocol.

MATERIALS AND METHODS

Patients

The Dignity Health Institutional Review Board approved this retrospective study. All data were acquired as part of clinical standard of care scans conducted between October 2018 to March 2020. Informed consent was obtained from patients who participated in this clinical investigation. Inclusion criteria were the presence of glioblastoma, IDH wild type, WHO grade 4 (based on 2016 WHO classification of CNS tumors), patient age >18 years, availability of perfusion datasets for both LFA and MFA injections on the institutional PACS and the presence of contrast enhancing lesions on the scans. Patients with poor injection (n = 2) and missing dynamic data points (n = 4) were excluded. After applying these inclusion and exclusion criteria, a total of 52 patients were included in the analysis. All patients received

chemotherapy and radiation therapy within 3-10 weeks after surgery or biopsy. The time between the end of radiation and the date of the perfusion scan ranged from 3 weeks to 8 years.

MRI Protocol

All studies were performed at 3T (Signa HDxt, GE Healthcare). Using a gradient-echo sequence, the standard pre-contrast and post-contrast 3D anatomical T1-weighted images were obtained with the following parameters: TE: 2.7 ms, TR: 7.1 ms, acquisition matrix: 512 x 512, voxel size: 1.0 x 1.0 mm^2, slice thickness: 2.0 mm, 212 axial slices, flip-angle: 13°. The LFA DSC-MRI with no preload was acquired using full-dose gadolinium-based contrast agent (gadobutrol, Gadavist) with the following scan parameters: TR: 1500 ms, TE: 30 ms, spatial resolution of 1.72 x 1.72 mm^2 (acquisition matrix: 128 x 128), slice thickness of 5 mm (20 axial slices), and pixel bandwidth of approximately 4 kHz. This injection served as the preload for the subsequent double-dose MFA acquisition. After a delay of 6 minutes, a second full dose of gadolinium was administered, and the MFA DSC-MRI was acquired with identical acquisition parameters except for a flip angle of 60°.

Data Analysis

All imaging data were postprocessed using the commercially available, FDA-cleared, OsiriX software plug-in, IB Clinic™. Standardized relative cerebral blood volume (sRCBV) maps were generated using IB Neuro™ (Imaging Biometrics, Version 21.12, Elm Grove, Wisconsin), by transforming the intensity histogram of each rCBV maps into a standard histogram and BSW leakage correction was applied to minimize T1 and T2* leakage effects.[23,38] The sRCBV maps were co-registered to the respective T1-weighted post-contrast images using IB Delta Suite™ (Imaging Biometrics, Version 21.05). A semi-automated analysis was performed using IB RadTech™ to determine the enhancing regions-of-interest (ROIs) on the ΔT1 (standardized post-contrast T1-weighted image – standardized pre-contrast T1-weighted image) maps, for each individual patient.

Statistical Analysis

The concordance correlation coefficient (CCC) between mean sRCBV derived from the LFA and MFA methods, and averaged across the entire 3D enhancing ROI, was determined to evaluate agreement. Additionally, we also calculated the CCC for each subject between the two protocols. Using MATLAB, reference FTB color class maps were computed from the MFA protocol with preload using the reference sRCBV thresholds, 1.0 and 1.56. The optimum sRCBV thresholds for the LFA protocol were determined by performing two separate ROC analyses on voxel-wise LFA-based sRCBV values. The analysis aimed to identify the thresholds that maximize the Youden Index (sensitivity + specificity – 1), by incorporating inverse weighting based on each patient's enhancing tumor volume, to address potential biases arising from variations in the ROI size. Thus, the application of these optimized thresholds yields single-dose, LFA-based FTB color class maps that best match those derived from the double-dose MFA reference protocol. Paired Wilcoxon signed rank tests were used to compare the sRCBV values between the LFA and MFA protocol. To compare the FTB maps between the two protocols, a Sørensen-Dice similarity coefficient was computed for each patient.

RESULTS

52 patients with grade IV glioblastoma were included in the study, including 24 females and 28 males (average age of 60 years; SD = 13, Range = 31 – 84).

Figure 1 shows the correlation between the mean sRCBV from the no-preload, LFA protocol and that determined from the MFA protocol with preload. The mean sRCBV was determined from the average of all voxels within the contrast-enhancing ROI, for both the protocols. Figure 2 shows the histogram of the voxel-wise CCC between the two protocols across all the patients, ranging from 0.52 to 0.96. A strong agreement between the two protocols is evident, with a CCC value of 0.98 for mean sRCBV, corroborating the prior, multi-site study.[39]

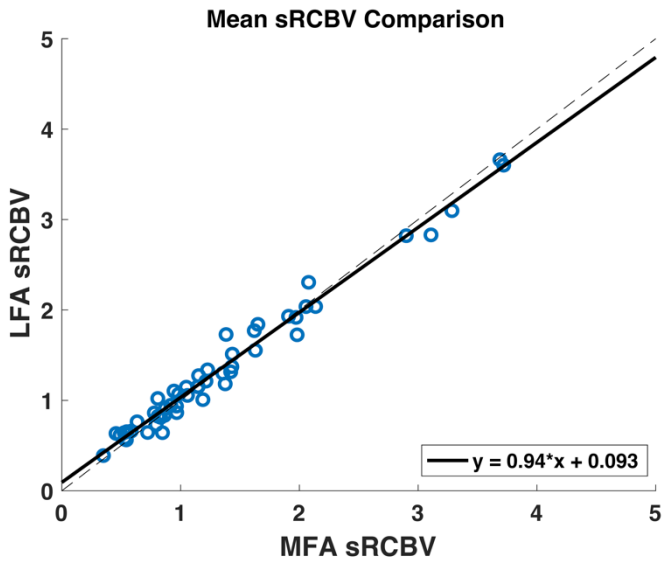

FIG 1. A sRCBV comparison between the single-dose, LFA protocol and the double-dose, MFA protocol on the mean tumor ROI across all the patients (n = 52) included in the study. This result shows a strong agreement between the two protocols with a concordance correlation coefficient value of 0.99.

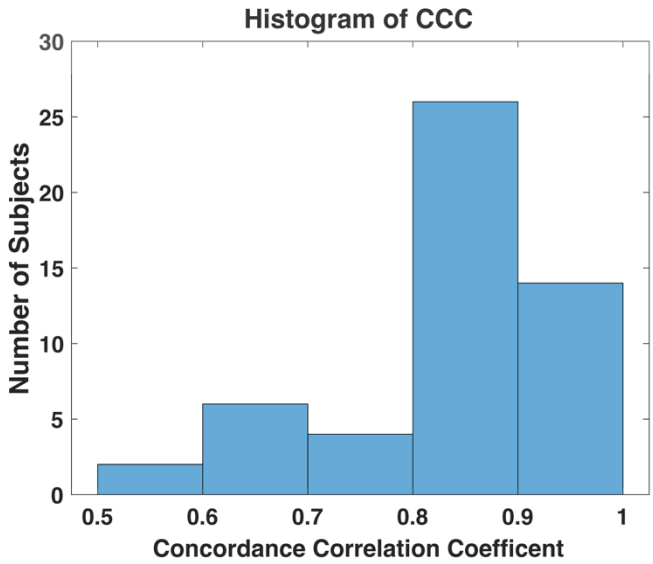

FIG 2. Histogram of concordance correlation coefficient across each patient, ranging from 0.52 to 0.96. 77% of patients exhibits a CCC greater than 0.8.

The optimal LFA thresholds for FTB mapping were identified through ROC analysis of voxel-wise sRCBV values across all patients. In comparison with the MFA thresholds 1.0 and 1.56, the optimum LFA thresholds corresponding to maximum Youden Index were determined to be 1.0 and 1.37, respectively. The area under the ROC for sRCBV < 1.0 and sRCBV > 1.56 was 0.95 and 0.96, respectively (Figure 3). A lower LFA threshold of 1.0 distinguished PTRE from tumor with sensitivity of 87.77% and and specificity 90.22%.

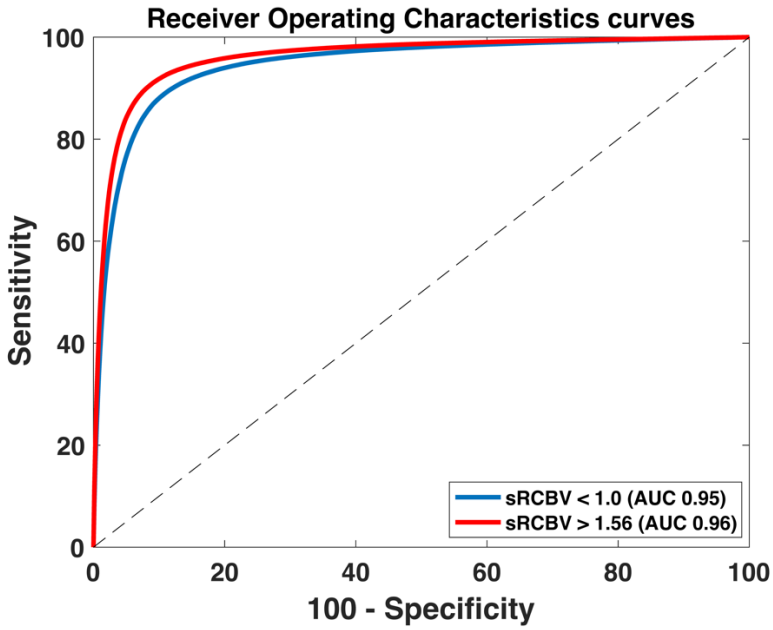

FIG 3. The area under the ROC curve for the optimal LFA-based thresholds is found to be 0.95 and 0.96 for sRCBV < 1.0 and > 1.56, respectively.

Prior studies have used 1.56 as the sRCBV upper reference threshold for the standard MFA protocol to identify aggressive tumor regions.[27,29,30] In this study, an upper threshold of 1.37 was identified for the LFA protocol with sensitivity of 90.87% and specificity of 91.10%. As shown in Figure 4, the mean and standard deviation of the fractional tumor burden (ratio of the number of enhancing voxels with sRCBV > 1 to the number of enhancing voxels) across all patients was 42.29% and 23.32% for MFA and 42.76% and 23.21% for LFA protocol, respectively. Based on this figure, it can be inferred that every patient exhibited some degree of tumor recurrence in the standard double-dose MFA protocol, with a median value of 40.82% (min: 6.44%; max: 94.35%). Since the percentage of tumor voxels for both LFA and MFA were non-normally distributed, as per Shapiro-Wilk test, a paired Wilcoxon signed rank test ($p = 0.36$) revealed no statistically significant difference between LFA and MFA tumor voxels.

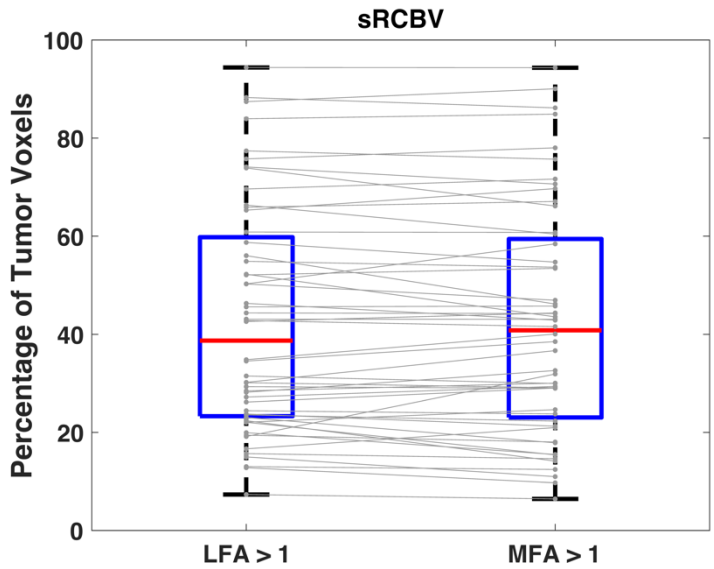

FIG 4. Boxplots (with individual datapoints) showing the consistency between percentage of tumor voxels (sRCBV > 1.0) in the enhancing tumor for the double-dose, MFA and single-dose, LFA protocol.

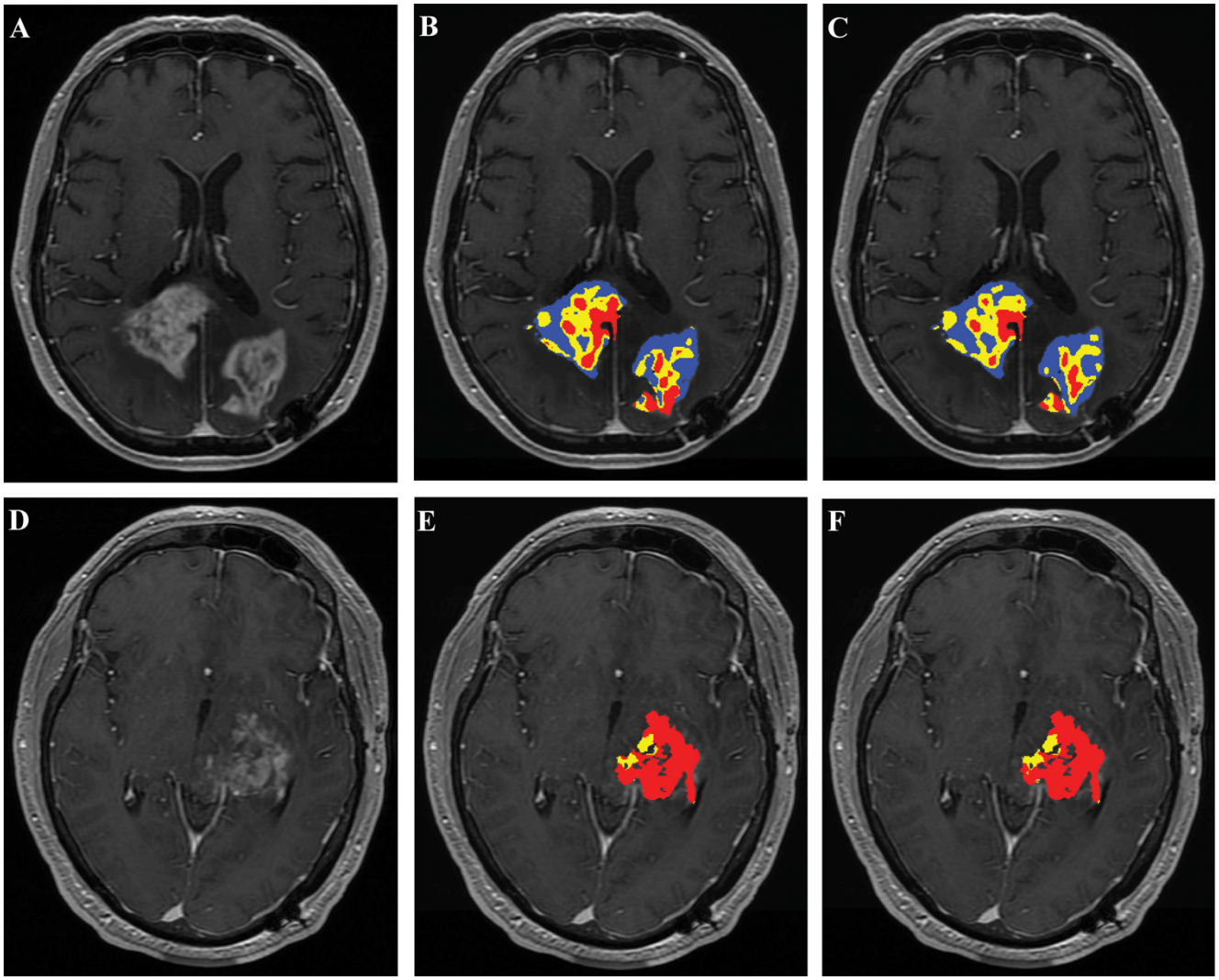

FIG 5. Patient (A-C) is a 73-year-old female with grade IV GBM presenting 15 months after surgical resection. Patient (D-F) is a 34-year-old male with grade IV GBM presenting 20 months after surgical resection. Images include anatomic post-contrast T1-weighted images (A, D), FTB maps for the single-dose, LFA protocol (B, E), using 1.0 and 1.37 and the reference double-dose, MFA protocol (C, F), using 1.0 and 1.56 superimposed on the contrast-enhanced T1-weighted images. Blue, yellow and red voxels represent PTRE (FTB_{low}, sRCBV < 1.0), tumor / treatment effect admixture (FTB_{mid}, 1.0 > sRCBV < 1.37 [LFA], 1.56 [MFA]) and high tumor cell probability (FTB_{high}, sRCBV > 1.37 [LFA], 1.56 [MFA])), respectively. The dice similarity coefficients comparing the LFA and MFA sRCBV for PTRE and tumor for patient A are 0.85 and 0.87, respectively. For patient D, the coefficients are 0.77 for PTRE and 0.96 for tumor.

Figure 5 shows representative post-contrast T1-weighted images depicting the enhancing tumor and the corresponding FTB maps for the LFA protocol (computed using the optimum thresholds derived from the ROC analysis, 1.0 and 1.37) and the MFA protocol (computed using the reference thresholds, 1.0 and 1.56). Figure 6 displays the histogram of the dice similarity coefficient across each patient for regions of PTRE (sRCBV < 1.0) and tumor (sRCBV > 1.0). The dice value for PTRE ranges from 0.71 to 0.98, while for tumor, it ranges from 0.46 to 0.98. The FTB maps for the subject with low dice value are shown in Figure S1 (supplementary material).

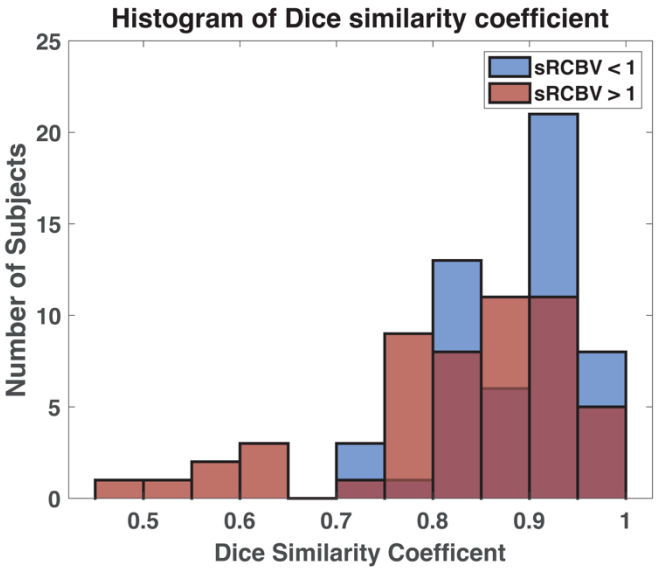

FIG 6. Histogram of dice similarity coefficient between the regions of PTRE (sRCBV < 1.0) and tumor (sRCBV > 1.0) for each patient. 92% and 67% of the subjects show a dice similarity coefficient greater than 0.8 for sRCBV < 1.0 and sRCBV > 1.0, respectively.

DISCUSSION

With increased adoption of the new consensus recommendations for DSC-MRI acquisition and analysis protocols, the role of DSC-MRI in distinguishing tumor recurrence and treatment effects is growing. Although the MFA protocol with preload is known to produce robust rCBV maps, it does incur additional cost and adds a potential source of variability, due to potential differences in incubation time between the preload and bolus injection. By leveraging a patient-based and validated DSC-MRI digital reference object, Semmineh et al. demonstrated that a protocol consisting of a single bolus injection (with no preload) and a LFA provided comparable rCBV accuracy across field strengths while reducing the contrast agent dosage and maintaining the brain tumor imaging protocol compliance.[40] The proposed LFA protocol was next validated in a multi-site study, which found a CCC between sRCBV values obtained using LFA without preload and MFA with preload of 0.96.[39] In this single-site study we corroborated the strong agreement between the LFA and MFA mean tumor sRCBV values (CCC = 0.99).

FTB maps offer a spatial quantification of both tumor and treatment effects, which often coexist within a lesion.[28] To determine the sRCBV threshold, we utilized FDA-cleared, clinically available software that computes standardized, leakage-corrected rCBV maps from DSC-MRI data. Previous studies have demonstrated that normalized and standardized rCBV maps have similar predictive performance.[24,25] However, the standardization technique eliminates the need for user dependent ROIs, necessary for normalization, and can be applied across field strengths and vendors, thereby improving rCBV reproducibility across patients and sites.[23,25]

Previous studies have published a wide range of rCBV thresholds to distinguish between recurrent tumor and treatment effects.[31] However, using MFA acquisition protocols consistent with the DSC-MRI consensus recommendation,[37] a lower threshold of 1.0 to distinguish pure PTRE (< 1.0) from the presence of tumor (>1.0) has been validated by two independent studies using image guided histopathology.[27,28] Use of this lower threshold to distinguish PTRE from tissue comprised of tumor has been emphasized in this study when using the LFA acquisition methods.

What remains less clear is which upper threshold to use with FTB maps to distinguish highly vascular tumor from tumor with intermediate sRCBV values. In the post-treatment setting, there is wide variability in the degree of microvascular proliferation of recurrent tumor. Invasive tumor or tumor with microscopic admixture with treatment effect may result in moderate values above 1.0, but not in the highly elevated range. Meanwhile, bulk tumor with high microvascular proliferation may result in markedly elevated rCBV. Using a normalized rCBV threshold of 1.75 to distinguish moderate vs. high rCBV has been shown to be helpful for predicting overall survival.[22] Though this threshold was originally identified for prognostic purposes, it has also been used as an upper threshold for the creation of the FTB class maps demonstrating clinical relevance.[35,41] Alternatively, the sRCBV upper threshold of 1.56 is based on the histopathology results indicating a 88% probability for detecting tumor cells.[27] In the present study, an optimal upper threshold for LFA acquisition was identified in reference to the 1.56 threshold.[27,29,30] The ROC analysis identified 1.0 as the lower threshold and 1.37 as the optimum upper threshold that yielded maximum Youden Index for 1.0 and 1.56 reference thresholds, respectively. Given the variability in the size of the enhancing ROI among the patients, the ROC analysis incorporated inverse weighting based on the size of each patients enhancing tumor volume. Despite applying thresholds of 1.0 and 1.37 for the LFA protocol, dice values tend to be low in patients with small enhancing ROIs, primarily with resection cavities, due to the limited number of voxels available. However, the clinical interpretations of the two maps remains consistent (predominantly PTRE).

In conclusion, this study demonstrates that the single-dose, LFA protocol is a reliable method for distinguishing between tumor and PTRE. There are several limitations that are inherent with this type of retrospective study. In particular, the scope of clinical information acquired and available for analysis is variable, including incomplete clinical-radiological follow-up and pathological analysis of patients who may have undergone a second surgery/biopsy. A potential limitation of the study is the absence of histopathology correlation, despite using the well-validated MFA protocol based FTB maps as a reference. However, we acknowledge that the reported sensitivity and specificity should be interpreted in regard to how well the LFA based FTB maps agree with the MFA based FTB maps and not necessarily

histopathologic ground truth. Similarly, future studies should validate the correlation between the derived LFA-based upper thresholds, radiographic progression and patient prognosis. Clinically, it would be compelling to also evaluate whether LFA-based FTB maps impact patient care (i.e. tumor board decisions) as it reduces the preload dose of gadolinium injection and eliminates the potential error arising from variations in contrast agent incubation time and dosing. Even though data for this retrospective study was acquired on a single MRI scanner, the previous consensus protocol study performed across multiple scanners and multiple sites established the strong agreement between the single-dose, low flip angle and double-dose, moderate flip angle protocols.[39] The focus of this study was to identify the thresholds for robust FTB mapping; specifically those that demarcate treatment effects from tumor recurrence and identify regions with a high probability of viable tumor cells.[24,26,27] Given the limited sample size included in this study, the upper threshold could vary with a different population. Thus, the prospective validation of the thresholds in a larger study, and including image-guided histopathology, is a future research area to promote clinical adoption.

CONCLUSIONS

This study provides experimental evidence showing that LFA FTB mapping can reliably distinguish tumor recurrence from treatment effects. This study provides further motivation for the use of the no-preload LFA protocol in the management of patients with glioblastoma.

ACKNOWLEDGMENTS

We would like to acknowledge Belinda Gutierrez for helping us obtain the data.

REFERENCES

1. Stupp R, Weller M, Belanger K, et al. Radiotherapy plus Concomitant and Adjuvant Temozolomide for Glioblastoma. *The New England Journal of Medicine*. Published online 2005.
2. Clarke JL, Chang S. Pseudoprogression and pseudoresponse: Challenges in brain tumor imaging. *Curr Neurol Neurosci Rep*. 2009;9(3):241-246. doi:10.1007/s11910-009-0035-4
3. Brandsma D, Van Den Bent MJ. Pseudoprogression and pseudoresponse in the treatment of gliomas. *Current Opinion in Neurology*. 2009;22(6):633-638. doi:10.1097/WCO.0b013e328332363e
4. Ellingson BM, Chung C, Pope WB, Boxerman JL, Kaufmann TJ. Pseudoprogression, radionecrosis, inflammation or true tumor progression? challenges associated with glioblastoma response assessment in an evolving therapeutic landscape. *J Neurooncol*. 2017;134(3):495-504. doi:10.1007/s11060-017-2375-2
5. Hygino Da Cruz LC, Rodriguez I, Domingues RC, Gasparetto EL, Sorensen AG. Pseudoprogression and Pseudoresponse: Imaging Challenges in the Assessment of Posttreatment Glioma. *AJNR Am J Neuroradiol*. 2011;32(11):1978-1985. doi:10.3174/ajnr.A2397
6. Brandsma D, Stalpers L, Taal W, Sminia P, Van Den Bent MJ. Clinical features, mechanisms, and management of pseudoprogression in malignant gliomas. *The Lancet Oncology*. 2008;9(5):453-461. doi:10.1016/S1470-2045(08)70125-6
7. Hu LS, Hawkins-Daarud A, Wang L, Li J, Swanson KR. Imaging of intratumoral heterogeneity in high-grade glioma. *Cancer Letters*. 2020;477:97-106. doi:10.1016/j.canlet.2020.02.025
8. Qin D, Yang G, Jing H, Tan Y, Zhao B, Zhang H. Tumor Progression and Treatment-Related Changes: Radiological Diagnosis Challenges for the Evaluation of Post Treated Glioma. *Cancers*. 2022;14(15):3771. doi:10.3390/cancers14153771
9. Thust SC, Van Den Bent MJ, Smits M. Pseudoprogression of brain tumors. *Magnetic Resonance Imaging*. 2018;48(3):571-589. doi:10.1002/jmri.26171
10. Malik DG, Rath TJ, Urcuyo Acevedo JC, et al. Advanced MRI Protocols to Discriminate Glioma From Treatment Effects: State of the Art and Future Directions. *Front Radio*. 2022;2:809373. doi:10.3389/fradi.2022.809373
11. Kim YH, Oh SW, Lim YJ, et al. Differentiating radiation necrosis from tumor recurrence in high-grade gliomas: Assessing the efficacy of 18F-FDG PET, 11C-methionine PET and perfusion MRI. *Clinical Neurology and Neurosurgery*. 2010;112(9):758-765. doi:10.1016/j.clineuro.2010.06.005
12. Nael K, Bauer AH, Hormigo A, et al. Multiparametric MRI for Differentiation of Radiation Necrosis From Recurrent Tumor in Patients With Treated Glioblastoma. *American Journal of Roentgenology*. 2018;210(1):18-23. doi:10.2214/AJR.17.18003
13. Prager AJ, Martinez N, Beal K, Omuro A, Zhang Z, Young RJ. Diffusion and Perfusion MRI to Differentiate Treatment-Related Changes Including Pseudoprogression from Recurrent Tumors in High-Grade Gliomas with Histopathologic Evidence. *AJNR Am J Neuroradiol*. 2015;36(5):877-885. doi:10.3174/ajnr.A4218
14. Zhang J, Wang Y, Wang Y, et al. Perfusion magnetic resonance imaging in the differentiation between glioma recurrence and pseudoprogression: a systematic review, meta-analysis and meta-regression. *Quant Imaging Med Surg*. 2022;12(10):4805-4822. doi:10.21037/qims-22-32
15. Sugahara T, Korogi Y, Tomiguchi S, et al. Posttherapeutic Intraaxial Brain Tumor: The Value of Perfusion-sensitive Contrast-enhanced MR Imaging for Differentiating Tumor Recurrence from Nonneoplastic Contrast-enhancing Tissue. Published online 2000.
16. Wang L, Wei L, Wang J, et al. Evaluation of perfusion MRI value for tumor progression assessment after glioma radiotherapy: A systematic review and meta-analysis. *Medicine*. 2020;99(52):e23766. doi:10.1097/MD.0000000000023766
17. Fatterpekar GM, Galheigo D, Narayana A, Johnson G, Knopp E. Treatment-Related Change Versus Tumor Recurrence in High-Grade Gliomas: A Diagnostic Conundrum—Use of Dynamic Susceptibility Contrast-Enhanced (DSC) Perfusion MRI. *American Journal of Roentgenology*. 2012;198(1):19-26. doi:10.2214/AJR.11.7417
18. Shiroishi MS, Boxerman JL, Pope WB. Physiologic MRI for assessment of response to therapy and prognosis in glioblastoma. *Neuro Oncol*. 2016;18(4):467-478. doi:10.1093/neuonc/nov179
19. Hu LS, Eschbacher JM, Dueck AC, et al. Correlations between Perfusion MR Imaging Cerebral Blood Volume, Microvessel Quantification, and Clinical Outcome Using Stereotactic Analysis in Recurrent High-Grade Glioma. *AJNR Am J Neuroradiol*. 2012;33(1):69-76. doi:10.3174/ajnr.A2743
20. Gasparetto EL, Pawlak MA, Patel SH, et al. Posttreatment Recurrence of Malignant Brain Neoplasm: Accuracy of Relative Cerebral Blood Volume Fraction in Discriminating Low from High Malignant Histologic Volume Fraction. *Radiology*. 2009;250(3):887-896. doi:10.1148/radiol.2502071444
21. Schmainda KM, Prah M, Connelly J, et al. Dynamic-susceptibility contrast agent MRI measures of relative cerebral blood volume predict response to bevacizumab in recurrent high-grade glioma. *Neuro-Oncology*. 2014;16(6):880-888. doi:10.1093/neuonc/not216
22. Law M, Young RJ, Babb JS, et al. Gliomas: Predicting Time to Progression or Survival with Cerebral Blood Volume Measurements at Dynamic Susceptibility-weighted Contrast-enhanced Perfusion MR Imaging. *Radiology*. 2008;247(2):490-498. doi:10.1148/radiol.2472070898
23. Bedekar D, Jensen T, Schmainda KM. Standardization of relative cerebral blood volume (rCBV) image maps for ease of both inter- and intrapatient

comparisons. *Magnetic Resonance in Med*. 2010;64(3):907-913. doi:10.1002/mrm.22445
24. Hoxworth JM, Eschbacher JM, Gonzales AC, et al. Performance of Standardized Relative CBV for Quantifying Regional Histologic Tumor Burden in Recurrent High-Grade Glioma: Comparison against Normalized Relative CBV Using Image-Localized Stereotactic Biopsies. *AJNR Am J Neuroradiol*. 2020;41(3):408-415. doi:10.3174/ajnr.A6486
25. Prah MA, Stufflebeam SM, Paulson ES, et al. Repeatability of Standardized and Normalized Relative CBV in Patients with Newly Diagnosed Glioblastoma. *AJNR Am J Neuroradiol*. 2015;36(9):1654-1661. doi:10.3174/ajnr.A4374
26. Hu LS, Baxter LC, Smith KA, et al. Relative Cerebral Blood Volume Values to Differentiate High-Grade Glioma Recurrence from Posttreatment Radiation Effect: Direct Correlation between Image-Guided Tissue Histopathology and Localized Dynamic Susceptibility-Weighted Contrast-Enhanced Perfusion MR Imaging Measurements. *AJNR Am J Neuroradiol.* 2009;30(3):552-558. doi:10.3174/ajnr.A1377
27. Prah MA, Al-Gizawiy MM, Mueller WM, et al. Spatial discrimination of glioblastoma and treatment effect with histologically-validated perfusion and diffusion magnetic resonance imaging metrics. *J Neurooncol*. 2018;136(1):13-21. doi:10.1007/s11060-017-2617-3
28. Hu LS, Eschbacher JM, Heiserman JE, et al. Reevaluating the imaging definition of tumor progression: perfusion MRI quantifies recurrent glioblastoma tumor fraction, pseudoprogression, and radiation necrosis to predict survival. *Neuro-Oncology*. 2012;14(7):919-930. doi:10.1093/neuonc/nos112
29. Connelly JM, Prah MA, Santos-Pinheiro F, Mueller W, Cochran E, Schmainda KM. Magnetic Resonance Imaging Mapping of Brain Tumor Burden: Clinical Implications for Neurosurgical Management: Case Report. *Neurosurg open.* 2021;2(4). doi:10.1093/neuopn/okab029
30. Amidon RF, Santos-Pinheiro F, Straza M, et al. Case report: Fractional brain tumor burden magnetic resonance mapping to assess response to pulsed low-dose-rate radiotherapy in newly-diagnosed glioblastoma. *Front Oncol*. 2022;12:1066191. doi:10.3389/fonc.2022.1066191
31. Patel P, Baradaran H, Delgado D, et al. MR perfusion-weighted imaging in the evaluation of high-grade gliomas after treatment: a systematic review and meta-analysis. *Neuro-Oncology.* 2017;19(1):118-127. doi:10.1093/neuonc/now148
32. Hu LS, Baxter LC, Pinnaduwage DS, et al. Optimized Preload Leakage-Correction Methods to Improve the Diagnostic Accuracy of Dynamic Susceptibility-Weighted Contrast-Enhanced Perfusion MR Imaging in Posttreatment Gliomas. *AJNR Am J Neuroradiol*. 2010;31(1):40-48. doi:10.3174/ajnr.A1787
33. Paulson ES, Schmainda KM. Comparison of Dynamic Susceptibility-weighted Contrast-enhanced MR Methods: Recommendations for Measuring Relative Cerebral Blood Volume in Brain Tumors. *Radiology*. 2008;249(2):601-613. doi:10.1148/radiol.2492071659
34. Schmainda KM, Prah MA, Rand SD, et al. Multisite Concordance of DSC-MRI Analysis for Brain Tumors: Results of a National Cancer Institute Quantitative Imaging Network Collaborative Project. *AJNR Am J Neuroradiol*. 2018;39(6):1008-1016. doi:10.3174/ajnr.A5675
35. Iv M, Liu X, Lavezo J, et al. Perfusion MRI-Based Fractional Tumor Burden Differentiates between Tumor and Treatment Effect in Recurrent Glioblastomas and Informs Clinical Decision-Making. *AJNR Am J Neuroradiol*. Published online September 12, 2019:ajnr;ajnr.A6211v1. doi:10.3174/ajnr.A6211
36. Welker K, Boxerman J, Kalnin A, et al. ASFNR Recommendations for Clinical Performance of MR Dynamic Susceptibility Contrast Perfusion Imaging of the Brain. *AJNR Am J Neuroradiol*. 2015;36(6):E41-E51. doi:10.3174/ajnr.A4341
37. Boxerman JL, Quarles CC, Hu LS, et al. Consensus recommendations for a dynamic susceptibility contrast MRI protocol for use in high-grade gliomas. *Neuro-Oncology*. 2020;22(9):1262-1275. doi:10.1093/neuonc/noaa141
38. Boxerman JL, Schmainda KM, Weisskoff RM. Relative cerebral blood volume maps corrected for contrast agent extravasation significantly correlate with glioma tumor grade, whereas uncorrected maps do not. *AJNR Am J Neuroradiol.* 2006;27(4):859-67
39. 39. Schmainda KM, Prah MA, Hu LS, et al. Moving Toward a Consensus DSC-MRI Protocol: Validation of a Low–Flip Angle Single-Dose Option as a Reference Standard for Brain Tumors. *AJNR Am J Neuroradiol*. Published online March 28, 2019:ajnr;ajnr.A6015v1. doi:10.3174/ajnr.A6015
40. 40. Semmineh NB, Bell LC, Stokes AM, Hu LS, Boxerman JL, Quarles CC. Optimization of Acquisition and Analysis Methods for Clinical Dynamic Susceptibility Contrast MRI Using a Population-Based Digital Reference Object. *AJNR Am J Neuroradiol*. 2018;39(11):1981-1988. doi:10.3174/ajnr.A5827
41. 41. Kuo F, Ng NN, Nagpal S, et al. DSC Perfusion MRI–Derived Fractional Tumor Burden and Relative CBV Differentiate Tumor Progression and Radiation Necrosis in Brain Metastases Treated with Stereotactic Radiosurgery. *AJNR Am J Neuroradiol*. 2022;43(5):689-695. doi:10.3174/ajnr.A7501

SUPPLEMENTAL FILES

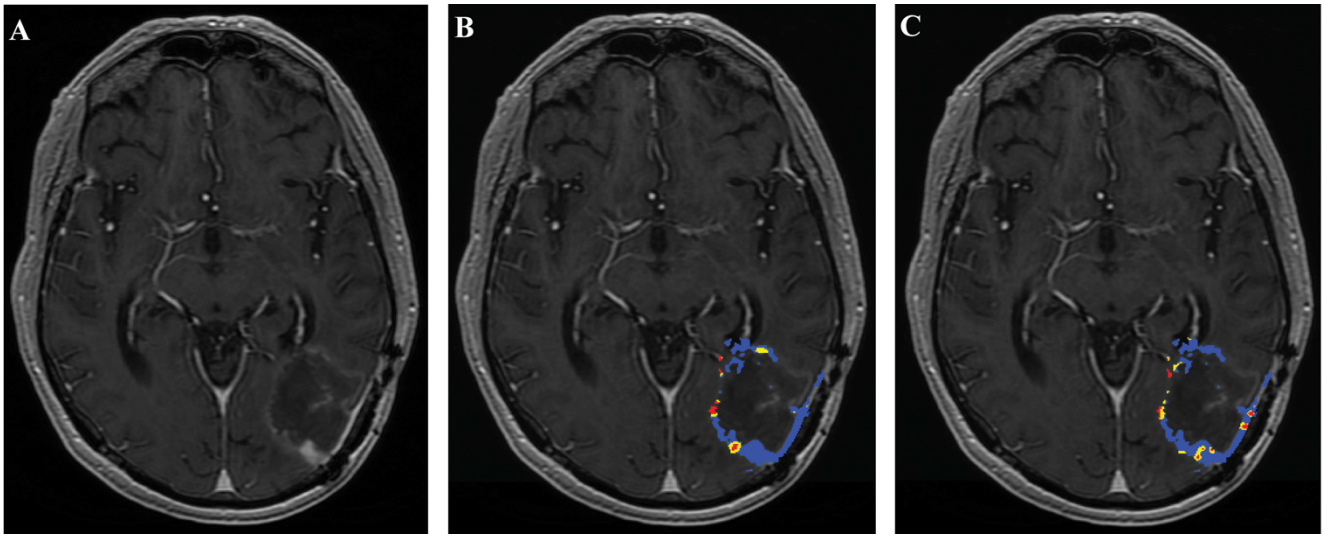

FIG S1. Patient (A-C) is a 62-year-old male with grade IV GM presenting 11 months after surgical resection with CCC value of 0.61 between the LFA and MFA sRCBV values. Post-contrast T1-weighted image (A), LFA FTB map (B) and MFA FTB map (C) superimposed on the post-contrast T1-image. The dice similarity coefficients comparing the LFA and MFA sRCBV for PTRE and tumor for Patient A are 0.88 and 0.46, respectively. Note the visual similarity of the maps despite low dice coefficients.